Electronic Supplementary Information (ESI)

Two 3D Porous Metal-Organic Frameworks with High Performance for Gas Adsorption and Separation

Shuo Yao, Dongmei Wang, Yu Cao, Guanghua Li, Qisheng Huo, and Yunling Liu*

State Key Laboratory of Inorganic Synthesis and Preparative Chemistry, College of Chemistry, Jilin University, Changchun 130012, P. R. China

Jilin University, Changchun 130012, P. R. China. E-mail: yunling@jlu.edu.cn; Fax: +86-431-85168624; Tel: +86-431-85168614

S1. Calculation procedures of selectivity from IAST

The measured experimental data is excess loadings (q^{ex}) of the pure components CO_2, CH_4, C_2H_6 and C_3H_8 for **JLU-Liu18**, which should be converted to absolute loadings (q) firstly.

$$q = q^{ex} + \frac{pV_{pore}}{ZRT}$$

Here Z is the compressibility factor. The Peng-Robinson equation was used to estimate the value of compressibility factor to obtain the absolute loading, while the measure pore volume 0.648 $cm^3\ g^{-1}$ is also necessary.

The dual-site Langmuir-Freundlich equation is used for fitting the isotherm data at 298K.

$$q = q_{m_1} \times \frac{b_1 \times p^{1/n_1}}{1 + b_1 \times p^{1/n_1}} + q_{m_2} \times \frac{b_2 \times p^{1/n_2}}{1 + b_2 \times p^{1/n_2}}$$

Here p is the pressure of the bulk gas at equilibrium with the adsorbed phase (kPa), q is the adsorbed amount per mass of adsorbent (mol kg^{-1}), q_{m1} and q_{m2} are the saturation capacities of sites 1 and 2 (mol kg^{-1}), b_1 and b_2 are the affinity coefficients of sites 1 and 2 (1/kPa), n_1 and n_2 are the deviations from an ideal homogeneous surface.

The selectivity of preferential adsorption of component 1 over component 2 in a mixture containing 1 and 2, perhaps in the presence of other components too, can be formally defined as

$$S = \frac{q_1/q_2}{p_1/p_2}$$

q_1 and q_2 are the absolute component loadings of the adsorbed phase in the mixture. These component loadings are also termed the uptake capacities. We calculate the values of q_1 and q_2 using the Ideal Adsorbed Solution Theory (IAST) of Myers and Prausnitz.

S2. Supporting Figures

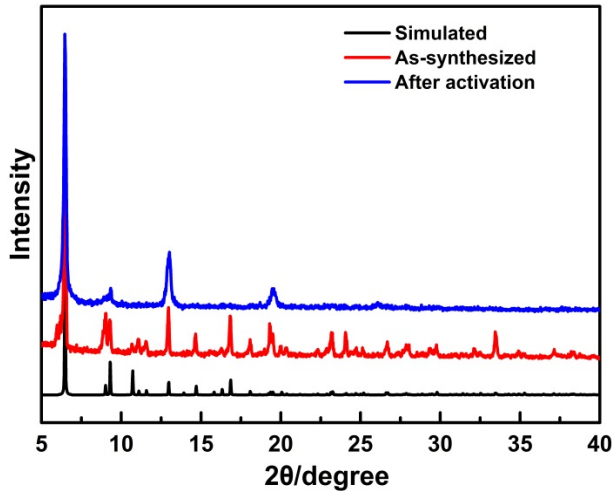

Fig. S1. PXRD patterns of **JLU-Liu18** for simulated, as-synthesized and activated samples. The differences in reflection intensity are probably due to preferred orientations in the powder sample.

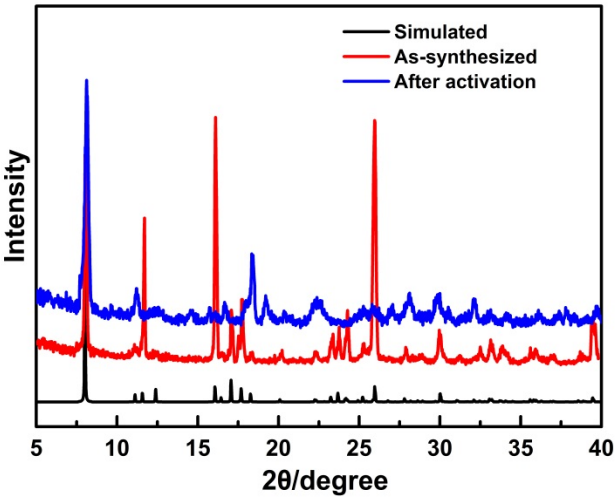

Fig. S2. PXRD patterns of **JLU-Liu19** for simulated, as-synthesized and activated samples. The differences in reflection intensity are probably due to preferred orientations in the powder sample.

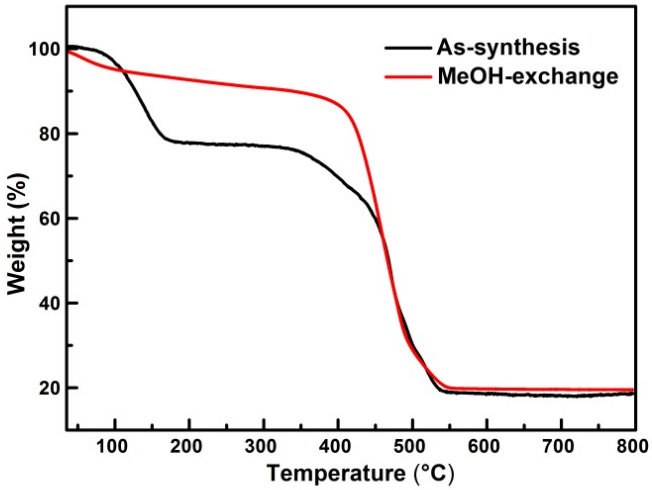

Fig. S3. Thermogravimetric analysis curves of **JLU-Liu18** for the as-synthesized and MeOH exchanged samples.

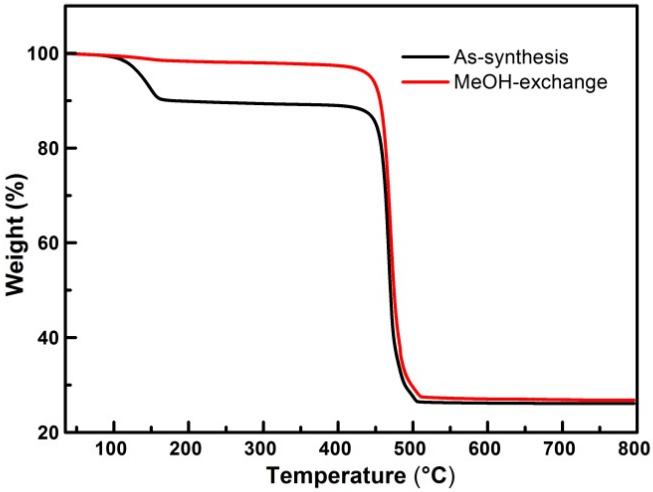

Fig. S4. Thermogravimetric analysis curves of **JLU-Liu19** for the as-synthesized and MeOH exchanged samples.

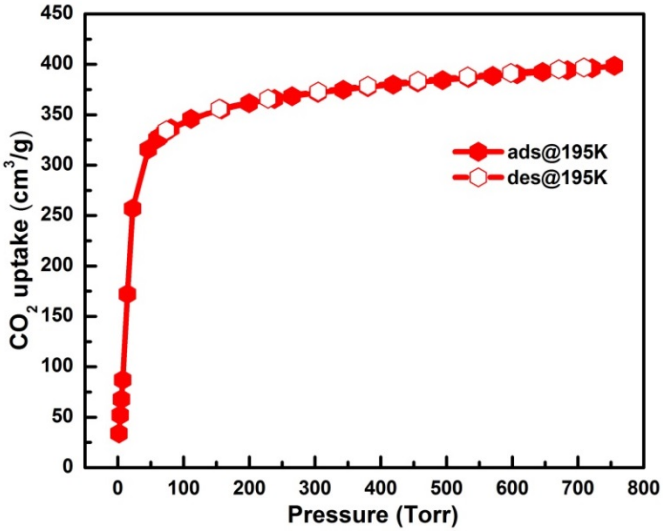

Fig. S5. The CO_2 isotherm for **JLU-Liu18** at 195 K under 1 bar.

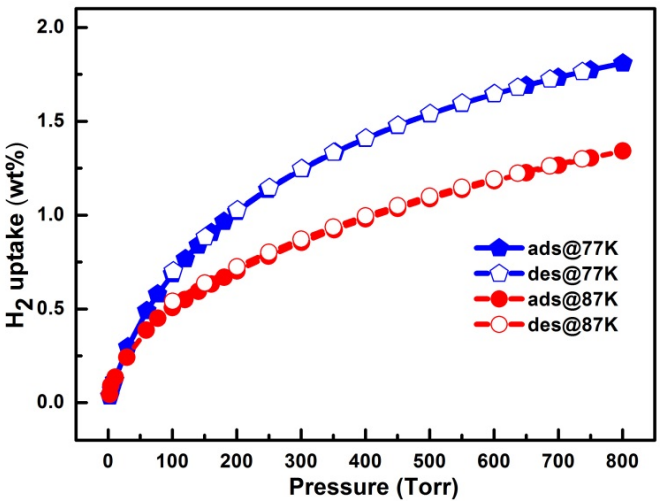

Fig. S6. The H_2 isotherm for **JLU-Liu18** at 77 (blue) and 87 K (red) under 1 bar.

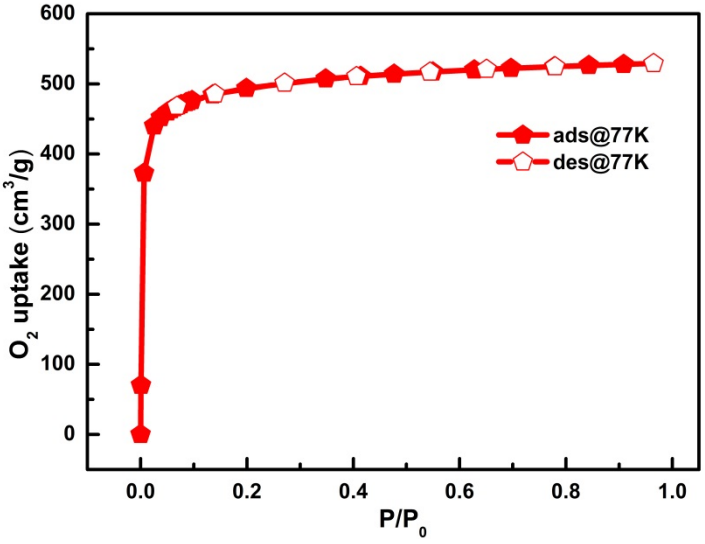

Fig. S7. The O_2 isotherms for **JLU-Liu18** at 77 K under 1 bar.

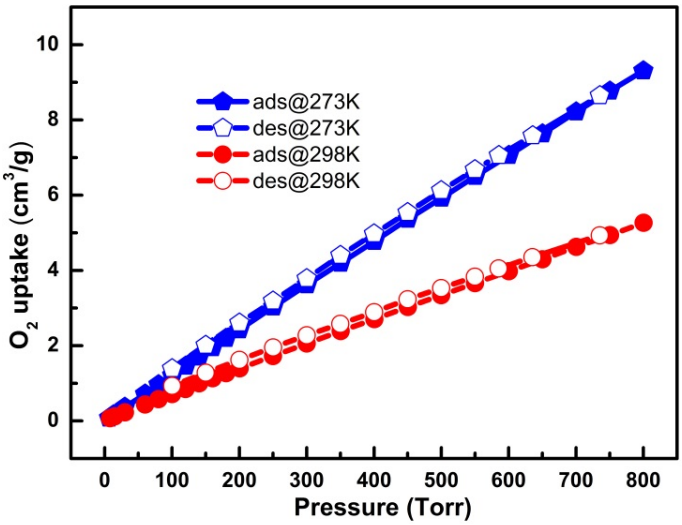

Fig. S8. The O_2 isotherms for **JLU-Liu18** at 273 and 298 K under 1 bar.

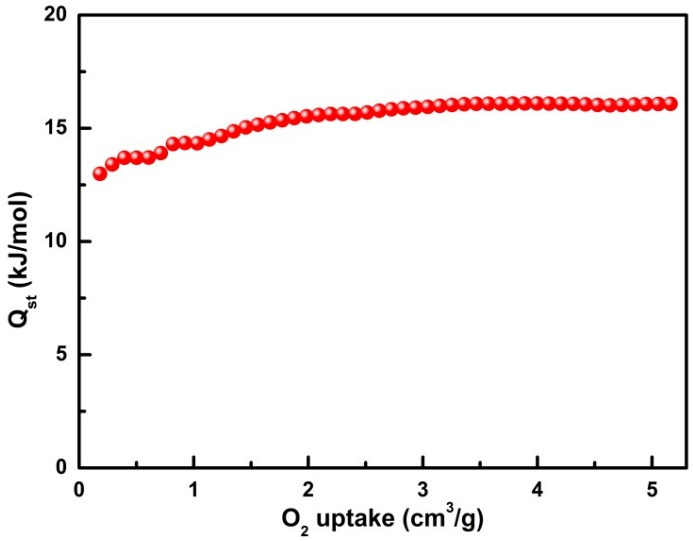

Fig. S9. Q_{st} of O_2 for **JLU-Liu18**.

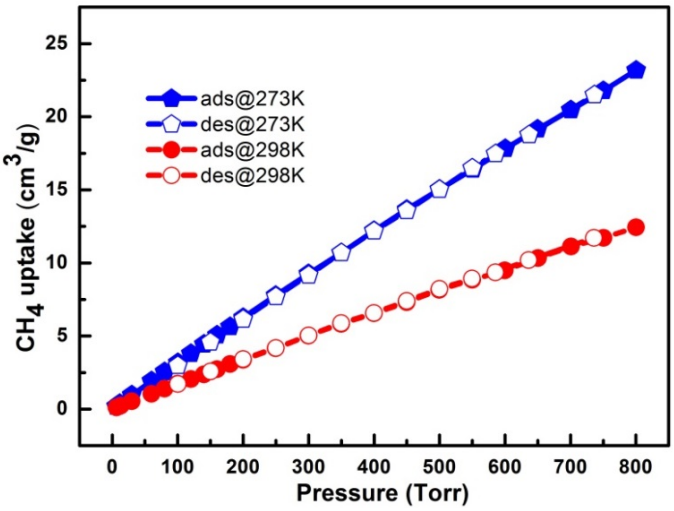

Fig. S10. The CH_4 isotherms for **JLU-Liu18** at 273 and 298 K under 1 bar.

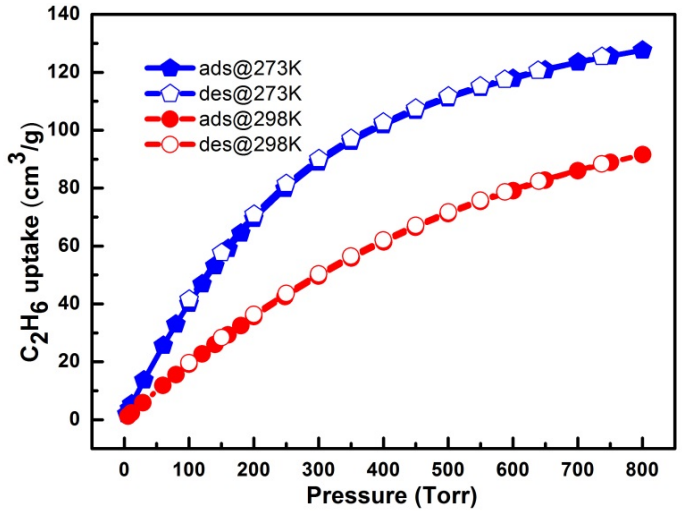

Fig. S11. The C_2H_6 isotherms for **JLU-Liu18** at 273 and 298 K under 1 bar.

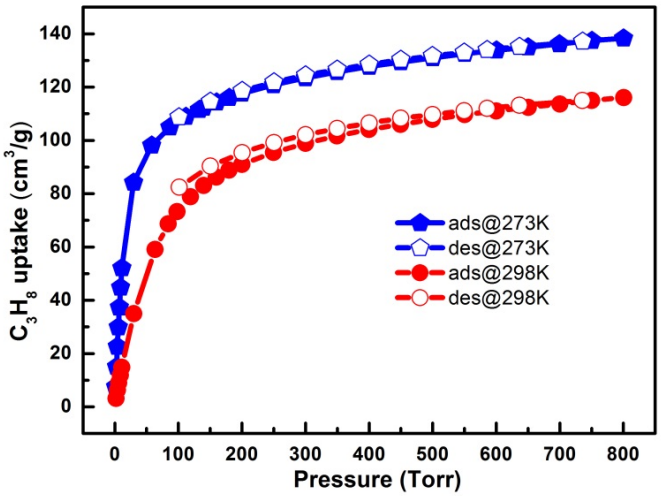

Fig. S12. The C_3H_8 isotherms for **JLU-Liu18** at 273 and 298 K.

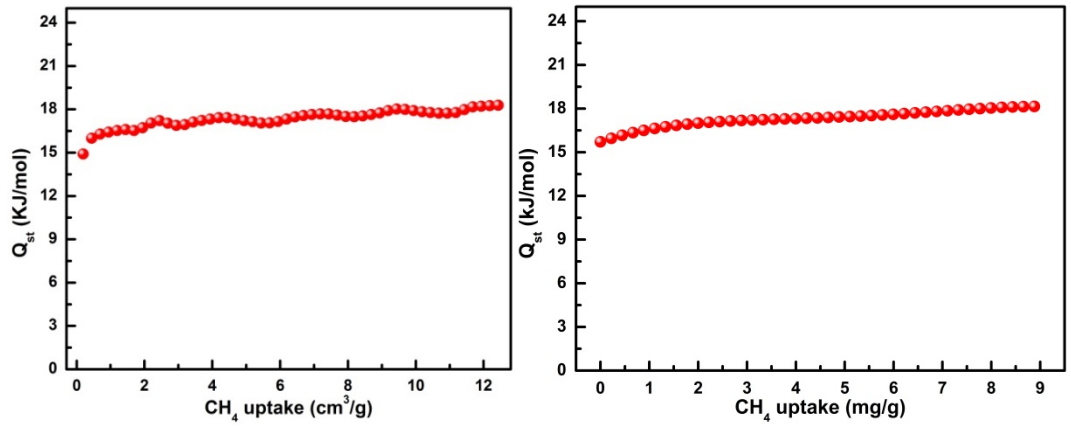

Fig. S13. Qst of CH_4 for **JLU-Liu18**. The left is calculated by MicroActive soft, while the right is calculated with virial method.

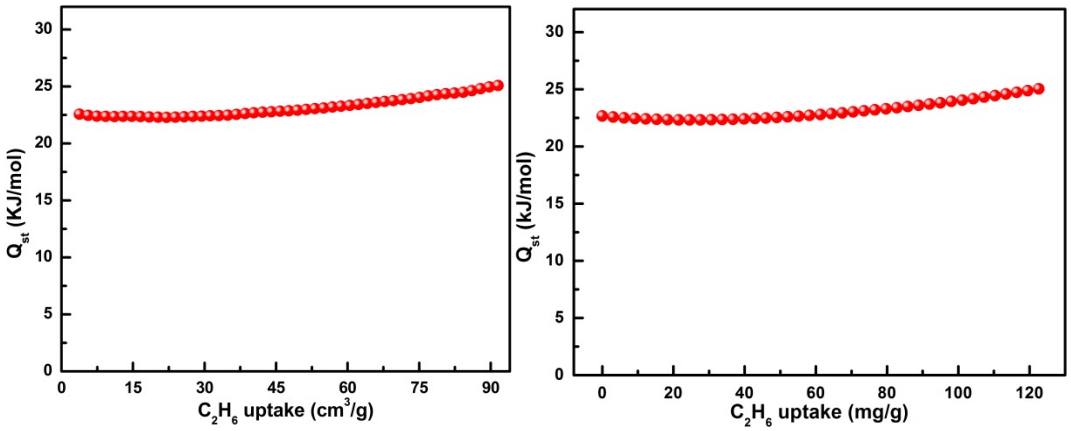

Fig. S14. Qst of C_2H_6 for **JLU-Liu18**. The left is calculated by MicroActive soft, while the right is calculated with virial method.

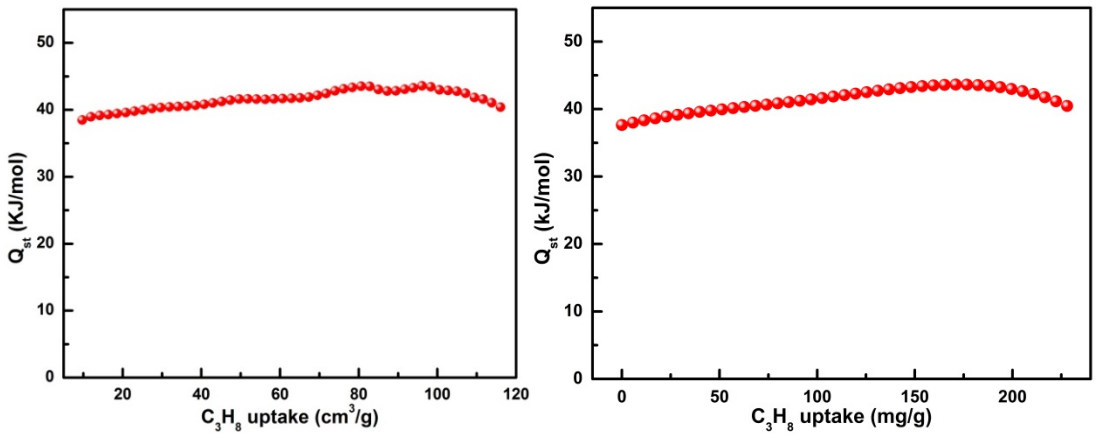

Fig. S15. Qst of C_3H_8 for **JLU-Liu18**. The left is calculated by MicroActive soft, while the right is calculated with virial method.

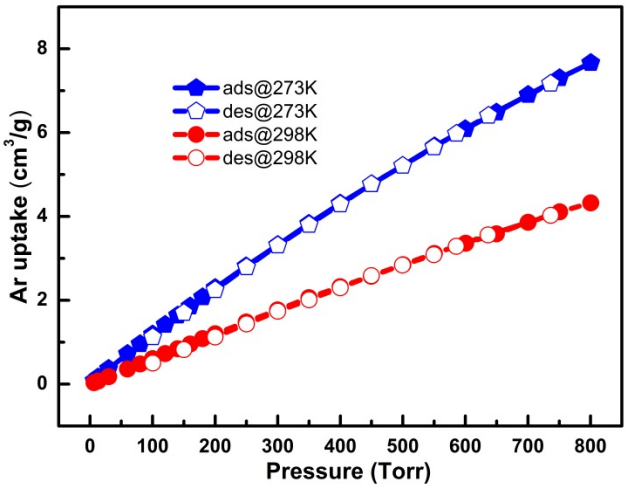

Fig. S16. Ar isotherms for **JLU-Liu18** at 273 and 298 K.

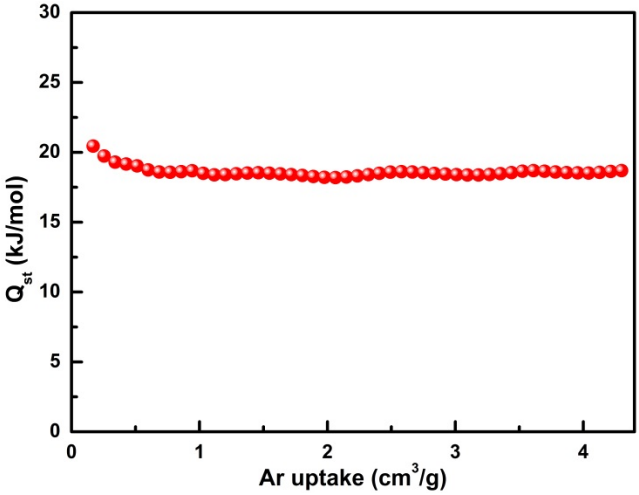

Fig. S17. Qst of Ar for **JLU-Liu18**.

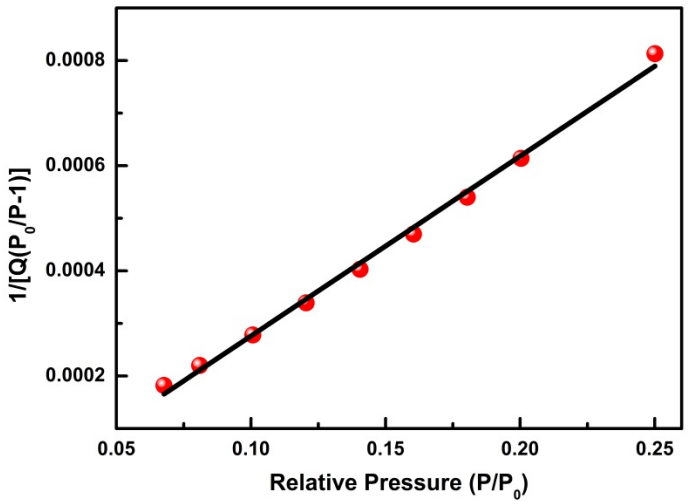

Fig. S18. The linear fitting curve for calculating BET surface areas of **JLU-Liu18**.

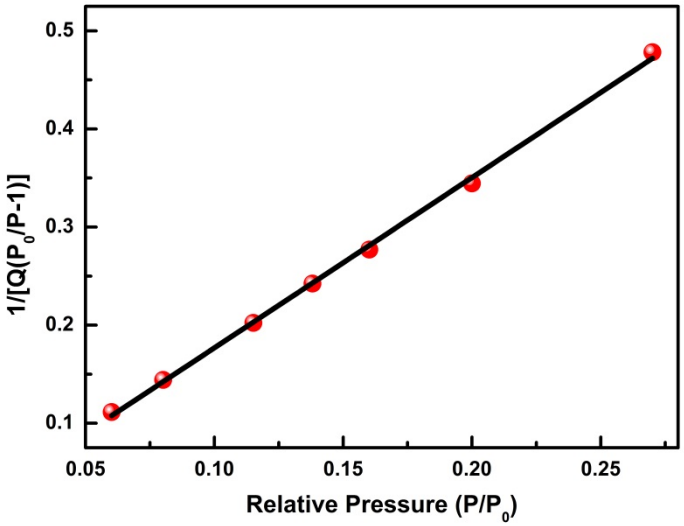

Fig. S19. The linear fitting curve for calculating BET surface areas of **JLU-Liu19**.

S3. Supporting Tables

Table S1. Crystal data and structure refinements for JLU-Liu18 and JLU-Liu19

compound	**JLU-Liu18**	**JLU-Liu19**
formula	$C_{69}\,H_{67}\,In_3\,N_8\,O_{23}$	$C_{20.5}\,H_{14.5}\,Cd\,N_{1.5}\,O_{4.5}$
Mw	1720.77	466.24
temp (K)	293(2)	293(2)
wavelength (Å)	0.71073	0.71073
Crystal system	trigonal	monoclinic,
space group	R-3c	C2/c
a (Å)	19.627(3)	16.709(3)
b (Å)	19.627(3)	15.867(3)
c (Å)	45.856(9)	8.0026(16)
V (Å^3)	15298(4)	1938.9(7)
Z, D_c (Mg/m^3)	6,1.121	4,1.597
F(000)	5208.0	928
θ range (deg)	1.49-25.85	2.57-25.09
reflns collected/unique	25368/3291	7049/1726
R_{int}	0.0320	0.0310
data/restraints/params	3291/0/117	1726/0/115
GOF on F^2	1.118	1.053
R_1, wR_2 (I>2σ(I))	0.0237,0.0694	0.0253,0.0627
R_1, wR_2 (all data)	0.0248, 0.0700	0.0315,0.0641

[a] $R_1 = \Sigma||F_o| - |F_c||/\Sigma|F_o|$, [b] $wR_2 = [\Sigma w(|F_o|^2 - |F_c|^2)/\Sigma|w(F_o^2)^2|]^{1/2}$

Table S2. Selected bond lengths [Å] and angles [º] for **JLU-Liu18**.

JLU-Liu18			
In(1)-O(3)	2.0289(3)	O(3)-In(1)-O(1)#4	94.38(4)
In(1)-O(2)#1	2.1592(13)	O(2)#1-In(1)-O(1)#4	92.49(6)
In(1)-O(2)#2	2.1593(13)	O(2)#2-In(1)-O(1)#4	87.24(6)
In(1)-O(1)#3	2.1763(12)	O(1)#3-In(1)-O(1)#4	171.24(7)
In(1)-O(1)#4	2.1764(13)	O(3)-In(1)-N(1)	180.000(1)
In(1)-N(1)	2.223(2)	O(2)#1-In(1)-N(1)	88.31(4)
O(1)-In(1)#5	2.1764(12)	O(2)#2-In(1)-N(1)	88.31(4)
O(2)-In(1)#2	2.1593(13)	O(1)#3-In(1)-N(1)	85.62(4)
O(3)-In(1)#6	2.0289(3)	O(1)#4-In(1)-N(1)	85.62(4)
O(3)-In(1)#7	2.0289(3)	C(10)-O(1)-In(1)#5	129.13(12)
O(3)-In(1)-O(2)#1	91.69(4)	C(10)-O(2)-In(1)#2	137.65(12)
O(3)-In(1)-O(2)#2	91.69(4)	In(1)#6-O(3)-In(1)#7	120.0
O(2)#1-In(1)-O(2)#2	176.62(7)	In(1)#6-O(3)-In(1)	120.0
O(3)-In(1)-O(1)#3	94.38(4)	In(1)#7-O(3)-In(1)	120.0
O(2)#1-In(1)-O(1)#3	87.25(6)	C(1)#8-N(1)-In(1)	120.80(11)
O(2)#2-In(1)-O(1)#3	92.50(6)	C(1)-N(1)-In(1)	120.80(11)

Symmetry transformations used to generate equivalent atoms:
#1 x+1/3,x-y+2/3,z+1/6 #2 -x+1,-y+1,-z+1 #3 -x+y+1/3,y-1/3,z+1/6 #4 x-y+1,x,-z+1 #5 y,-x+y+1,-z+1 #6 -x+y+1,-x+1,z #7 -y+1,x-y,z #8 -x+4/3,-x+y+2/3,-z+7/6

Table S3. Selected bond lengths [Å] and angles [º] for **JLU-Liu19**.

JLU-Liu19			
Cd(1)-O(1)#1	2.206(2)	O(1)#1-Cd(1)-O(2)#3	105.34(9)
Cd(1)-O(1)	2.206(2)	O(1)-Cd(1)-O(2)#3	83.13(9)
Cd(1)-N(1)#2	2.264(3)	N(1)#2-Cd(1)-O(2)#3	83.84(5)
Cd(1)-O(2)#3	2.475(3)	O(1)#1-Cd(1)-O(2)#4	83.13(9)
Cd(1)-O(2)#4	2.475(3)	O(1)-Cd(1)-O(2)#4	105.34(9)
O(2)-Cd(1)#4	2.412(4)	N(1)#2-Cd(1)-O(2)#4	83.84(5)
N(2)-Cd(1)-N(2)#1	2.475(3)	O(2)#3-Cd(1)-O(2)#4	167.67(10)
N(1)-Cd(1)#6	2.264(3)	C(10)-O(1)-Cd(1)	103.3(2)
O(1)#1-Cd(1)-O(1)	95.09(13)	C(10)-O(2)-Cd(1)#4	125.0(2)
O(1)#1-Cd(1)-N(1)#2	132.45(7)	C(1)#5-N(1)-Cd(1)#6	120.62(16)
O(1)-Cd(1)-N(1)#2	132.45(7)	C(1)-N(1)-Cd(1)#6	120.62(16)

Symmetry transformations used to generate equivalent atoms:
#1 -x+1,y,-z+3/2 #2 x+1/2,y-1/2,z+1 #3 x,-y,z+1/2 #4 -x+1,-y,-z+1 #5 -x,y,-z-1/2 #6 x-1/2,y+1/2,z-1

Table S4. The CO_2 adsorption information of representative In-MOFs.

Compound	298 K (cm^3/g)	273 K (cm^3/g)	195 K (cm^3/g)	Ref.
JLU-Liu18	63	129	400	This work
437-MOF	N.A.	N.A.	607	1
CPM-6	65	106.7	N.A.	2
CPM-5	54.5	81.3	N.A.	2
$(Et_4N)_3[In_3(btc)_4]\cdot DEF$	N.A.	28.9	N.A.	3
$(choline)_3[In_3(btc)_4]\cdot 2DMF$	N.A.	70.6	N.A.	3
$(In_3O)(OH)(ADC)_2(NH_2IN)_2\cdot 2.67H_2O$	72.1	N.A.	437	4
$(In_3O)(OH)(ADC)_2\cdot 4.67H_2O$	67.2	N.A.	388	4
CPM-20	47.7	91.2	N.A.	5
CPM-19-Nd	N.A.	38.4	N.A.	5
MMPF-8	47	82	N.A.	6
MMPF-7	34	55	N.A.	6
CPM-12	N.A.	78.6	N.A.	7
CPM-13	N.A.	45.4	N.A.	7
InOF-8	N.A.	66.2	N.A.	8
FJI-C1	41.2	64.0	427.5	9

N.A.: Not Available. The articles do not list the data.

Reference:

1. M. Du, M. Chen, X. G. Yang, J. Wen, X. Wang, S.-M. Fang and C.-S. Liu, *J. Mater. Chem. A*, 2014, **2**, 9828-9834.
2. S. T. Zheng, J. T. Bu, Y. Li, T. Wu, F. Zuo, P. Feng and X. Bu, *J. Am. Chem. Soc.*, 2010, **132**, 17062-17064.
3. S. Chen, J. Zhang, T. Wu, P. Feng and X. Bu, *J. Am. Chem. Soc.*, 2009, **131**, 16027-16029.
4. X. Gu, Z. H. Lu and Q. Xu, *Chem. Commun.*, 2010, **46**, 7400-7402.
5. S. T. Zheng, T. Wu, C. Chou, A. Fuhr, P. Feng and X. Bu, *J. Am. Chem. Soc.*, 2012, **134**, 4517-4520.
6. W. Y. Gao, Z. Zhang, L. Cash, L. Wojtas, Y. S. Chen and S. Ma, *CrystEngComm*, 2013, **15**, 9320-9323.
7. S. T. Zheng, J. J. Bu, T. Wu, C. Chou, P. Feng and X. Bu, *Angew Chem. Int. Ed.*, 2011, **50**, 8858-8862.
8. J. Qian, F. Jiang, K. Su, J. Pan, Z. Xue, L. Liang, P. P. Bag and M. Hong, *Chem. Commun.*, 2014, **50**, 15224-15227.
9. Y. Huang, Z. Lin, H. Fu, F. Wang, M. Shen, X. Wang and R. Cao, *ChemSusChem*, 2014, **7**, 2647-2653.

Table S5. The refined parameters for the Dual-site Langmuir-Freundlich equations fit for the pure isotherms of CO_2, CH_4, C_2H_6 and C_3H_8 for **JLU-Liu18** at 298 K.

	q_{m1}	b_1	n_1	q_{m2}	b_2	n_2	R^2
CO_2	0.26696	6.18812E-7	3.62986	24.64042	7.90917E-4	1.08137	0.999996
CH_4	0.00156	0.33719	2.75287	4.28409	0.00125	1.01179	0.999930
C_2H_6	4.53312	0.01554	0.98626	1.92566	5.58682E-4	1.76187	0.999998
C_3H_8	51.44651	0.00399	0.43988	3.68154	0.07234	1.38053	0.999970